Human demographic history impacts genetic risk prediction across diverse populations

Alicia R. Martin[1,2,3], Christopher R. Gignoux[3], Raymond K. Walters[1,2], Genevieve L. Wojcik[3], Benjamin M. Neale[1,2], Simon Gravel[4], Mark J. Daly[1,2], Carlos D. Bustamante[3], Eimear E. Kenny[5]

[1] Analytic and Translational Genetics Unit, Massachusetts General Hospital, Boston, MA 02114

[2] Medical and Population Genetics, Broad Institute of Harvard and the Massachusetts Institute of Technology, Cambridge, MA USA

[3] Department of Genetics, Stanford University, Stanford, CA 94305, USA

[4] Department of Human Genetics, McGill University, Montreal, Quebec, Canada

[5] Department of Genetics and Genomic Sciences, Mt. Sinai School of Medicine, New York, NY, USA

Corresponding author: eimear.kenny@mssm.edu

Abstract (250 words)

The vast majority of genome-wide association studies are performed in Europeans, and their transferability to other populations is dependent on many factors (e.g. linkage disequilibrium, allele frequencies, genetic architecture). As medical genomics studies become increasingly large and diverse, gaining insights into population history and consequently the transferability of disease risk measurement is critical. Here, we

disentangle recent population history in the widely-used 1000 Genomes Project reference panel, with an emphasis on populations underrepresented in medical studies. To examine the transferability of single-ancestry GWAS, we used published summary statistics to calculate polygenic risk scores for six well-studied traits and diseases. We identified directional inconsistencies in all scores; for example, height is predicted to decrease with genetic distance from Europeans, despite robust anthropological evidence that West Africans are as tall as Europeans on average. To gain deeper quantitative insights into GWAS transferability, we developed a complex trait coalescent-based simulation framework considering effects of polygenicity, causal allele frequency divergence, and heritability. As expected, correlations between true and inferred risk were typically highest in the population from which summary statistics were derived. We demonstrated that scores inferred from European GWAS were biased by genetic drift in other populations even when choosing the same causal variants, and that biases in any direction were possible and unpredictable. This work cautions that summarizing findings from large-scale GWAS may have limited portability to other populations using standard approaches, and highlights the need for generalized risk prediction methods and the inclusion of more diverse individuals in medical genomics.

Introduction

The majority of genome-wide association studies (GWAS) have been performed in populations of European descent[1-4]. An open question in medical genomics is the degree to which these results transfer to new populations. GWAS have yielded tens of

47 thousands of common genetic variants significantly associated with human medical and
48 evolutionary phenotypes, most of which have replicated in other ethnic groups[5-8].
49 However, GWAS are optimally powered to discover common variant associations, and
50 the European bias in GWAS results in associated SNPs with higher minor allele
51 frequencies on average compared to other populations. The predictive power of GWAS
52 findings in non-Europeans are therefore limited by population differences in allele
53 frequencies and linkage disequilibrium structure.
54
55 As GWAS sample sizes grow to hundreds of thousands of samples, they also become
56 better powered to detect rare variant associations[9-11]. Large-scale sequencing studies
57 have demonstrated that rare variants show stronger geographic clustering than
58 common variants[12-14]. Rare, disease-associated variants are therefore expected to track
59 with recent population demography and/or be population restricted[13,15-17]. As the next
60 era of GWAS expands to evaluate the disease-associated role of rare variants, it is not
61 only scientifically imperative to include multi-ethnic populations, it is also likely that such
62 studies will encounter increasing genetic heterogeneity in very large study populations.
63 A comprehensive understanding of the genetic diversity and demographic history of
64 multi-ethnic populations is critical for appropriate applications of GWAS, and ultimately
65 for ensuring that genetics does not contribute to or enhance health disparities[4].
66
67 The most recent release of the 1000 Genomes Project (phase 3) provides one of the
68 largest global reference panels of whole genome sequencing data, enabling a broad
69 survey of human genetic variation[18]. The depth and breadth of diversity queried

70 facilitates a deep understanding of the evolutionary forces (e.g. selection and drift)
71 shaping existing genetic variation in present-day populations that contribute to
72 adaptation and disease[19-25]. Studies of admixed populations have been particularly
73 fruitful in identifying genetic adaptations and risk for diseases that are stratified across
74 diverged ancestral origins[26-34]. Admixture patterns became especially complex during
75 the peopling of the Americas, with extensive recent admixture spanning multiple
76 continents. Processes shaping structure in these admixed populations include sex-
77 biased migration and admixture, isolation-by-distance, differential drift in mainland
78 versus island populations, and variable admixture timing[13,35,36].
79
80 Standard GWAS strategies approach population structure as a nuisance factor. A
81 typical step-wise procedure first detects dimensions of global population structure in
82 each individual, using principal component analysis (PCA) or other methods[37-40], and
83 often excludes “outlier” individuals from the analysis and/or corrects for inflation arising
84 from population structure in the statistical model for association. Such strategies reduce
85 false positives in test statistics, but can also reduce power for association in
86 heterogeneous populations, and are less likely to work for rare variant association[41-44].
87 Recent methodological advances have leveraged patterns of global and local ancestry
88 for improved association power[30,45,46], fine-mapping[47] and genome assembly[48]. At the
89 same time, population genetic studies have demonstrated the presence of fine-scale
90 sub-continental structure in the African, Native American, and European components of
91 populations from the Americas[49-52]. If trait-associated variants follow the same patterns

92 of demography, then we expect that modeling sub-continental ancestry may enable
93 their improved detection in admixed populations.
94
95 In this study, we explore the impact of population diversity on the landscape of variation
96 underlying human traits. We infer demographic history for the global populations in the
97 1000 Genomes Project, focusing particularly on admixed populations from the
98 Americas, which are under represented in medical genetic studies[4]. We disentangle
99 local ancestry to infer the ancestral origins of these populations. We link this work to
100 ongoing efforts to improve study design and disease variant discovery by quantifying
101 biases in clinical databases and GWAS in diverse and admixed populations. These
102 biases have a striking impact on genetic risk prediction; for example, a previous study
103 calculated polygenic risk scores for schizophrenia in East Asians and Africans based on
104 GWAS summary statistics derived from a European cohort, and found that prediction
105 accuracy was reduced by more than 50% in non-European populations[53]. To
106 disentangle the role of demography on polygenic risk prediction derived from single-
107 ancestry GWAS, we designed a novel coalescent-based simulation framework reflecting
108 modern human population history and show that polygenic risk scores derived from
109 European GWAS are biased when applied to diverged populations. Specifically, we
110 identify reduced variance in risk prediction with increasing divergence from Europe
111 reflecting decreased overall variance explained, and demonstrate that an enrichment of
112 low frequency risk and high frequency protective alleles contribute to an overall
113 protective shift in European inferred risk on average across traits. Our results highlight

114 the need for the inclusion of more diverse populations in GWAS as well as genetic risk
115 prediction methods improving transferability across populations.
116
117 **Material and Methods**
118 *Ancestry deconvolution*
119 We used the phased haplotypes from the 1000 Genomes consortium. We phased
120 reference haplotypes from 43 Native American samples from[54] inferred to have > 0.99
121 Native ancestry in ADMIXTURE using SHAPEIT2 (v2.r778)[55], then merged the
122 haplotypes using scripts made publicly available. These combined phased haplotypes
123 were used as input to the PopPhased version of RFMix v1.5.4[56] with the following flags:
124 -w 0.2, -e 1, -n 5, --use-reference-panels-in-EM, --forward-backward. The node size of 5
125 was selected to reduce bias in random forests resulting from unbalanced reference
126 panel sizes (AFR panel N=504, EUR panel N=503, and NAT panel N=43). We used the
127 default minimum window size of 0.2 cM to enable model comparisons with previously
128 inferred models using *Tracts*[57]. We used 1 EM iteration to improve the local ancestry
129 calls without substantially increasing computational complexity. We used the reference
130 panel in the EM to take better advantage of the Native American ancestry tracts from
131 the Hispanic/Latinos in the EM given the small NAT reference panel. We set the LWK,
132 MSL, GWD, YRI, and ESN as reference African populations, the CEU, GBR, FIN, IBS,
133 and TSI as reference European populations, and the samples from Mao et al[54] with
134 inferred > 0.99 Native ancestry as reference Native American populations, as
135 previously[58].
136

137 *Ancestry-specific PCA*

138 We performed ancestry-specific PCA, as described in[35]. The resulting matrix is not
139 necessarily orthogonalized, so we subsequently performed singular value
140 decomposition in python 2.7 using numpy. There were a small number of major outliers,
141 as seen previously[35]. There was one outlier (ASW individual NA20314) when analyzing
142 the African tracts, which was expected as this individual has no African ancestry. There
143 were 8 outliers (PUR HG00731, PUR HG00732, ACB HG01880, ACB HG01882, PEL
144 HG01944, ACB HG02497, ASW NA20320, ASW NA20321) when analyzing the
145 European tracts. Some of these individuals had minimal European ancestry, had South
146 or East Asian ancestry misclassified as European ancestry resulting from a limited 3-
147 way ancestry reference panel, or were unexpected outliers. As described in the
148 PCAmask manual, a handful of major outliers sometimes occur. As AS-PCA is an
149 iterative procedure, we therefore removed the major outliers for each sub-continental
150 analysis and orthogonalized the matrix on this subset.

151

152 *Tracts*

153 The RFMix output was collapsed into haploid bed files, and “UNK” or unknown ancestry
154 was assigned where the posterior probability of a given ancestry was < 0.90. These
155 collapsed haploid tracts were used to infer admixture timings, quantities, and
156 proportions for the ACB and PEL (new to phase 3) using *Tracts*[57]. Because the ACB
157 have a very small proportion of Native American ancestry, we fit three 2-way models of
158 admixture, including one model of single- and two models of double-pulse admixture
159 events, using *Tracts*. In both of the double-pulse admixture models, the model includes

160 an early mixture of African and European ancestry followed by another later pulse of
161 either European or African ancestry. We randomized starting parameters and fit each
162 model 100 times and compared the log-likelihoods of the model fits. The single-pulse
163 and double-pulse model with a second wave of African admixture provided the best fits
164 and reached similar log-likelihoods, with the latter showing a slight improvement in fit.
165
166 We next assessed the fit of 9 different models in *Tracts* for the PEL[57], including several
167 two-pulse and three-pulse models. Ordering the populations as NAT, EUR, and AFR,
168 we tested the following models: ppp_ppp, ppp_pxp, ppp_xxp, ppx_xxp, ppx_xxp_ppx,
169 ppx_xxp_pxx, ppx_xxp_pxp, ppx_xxp_xpx, and ppx_xxp_xxp, where the order of each
170 letter corresponds with the order of populations given above, an underscore indicates a
171 distinct migration event with the first event corresponding with the most generations
172 before present, p corresponding with a pulse of the ordered ancestries, and x
173 corresponding with no input from the ordered ancestries. We tested all 9 models
174 preliminarily 3 times, and for all models that converged and were within the top 3
175 models, we subsequently fit each model with 100 starting parameters randomizations.
176
177 *Imputation accuracy*
178 Imputation accuracy was calculated using a leave-one-out internal validation approach.
179 Two array designs were compared for this analysis: Illumina OmniExpress and
180 Affymetrix Axiom World Array LAT. Sites from these array designs were subset from
181 chromosome 9 of the 1000 Genomes Project Phase 3 release for admixed populations.

182 After fixing these sites, each individual was imputed using the rest of the dataset as a
183 reference panel.
184
185 Overall imputation accuracy was binned by minor allele frequency (0.5-1%, 1-2%, 2-3%,
186 3-4%, 4-5%, 5-10%, 10-20%, 20-30%, 30-40%, 40-50%) comparing the genotyped true
187 alleles to the imputed dosages. A second round of analyses stratified the imputation by
188 local ancestry diplotype, which was estimated as described earlier. Within each
189 ancestral diplotype (AFR_AFR, AFR_NAT, AFR_EUR, EUR_EUR, EUR_NAT,
190 NAT_NAT), imputation accuracy was again estimated within MAF bins.
191
192 *Empirical polygenic risk score inferences*
193 To compute polygenic risk scores in the 1000 Genomes samples using summary
194 statistics from previous GWAS, we first filtered to biallelic SNPs and removed
195 ambiguous AT/GC SNPs from the integrated 1000 Genome call set. To get relatively
196 independent associations taking LD into account when multiple significant p-value
197 associations are in the same region in a GWAS, we performed LD clumping in plink (--
198 clump) for all variants with MAF ≥ 0.01[59], which uses a greedy algorithm ordering SNPs
199 by p-value, then selectively removes SNPs within close proximity and LD in ascending
200 p-value order (i.e. starting with the most significant SNP). As a population cohort with
201 similar LD patterns to the study sets, we used European 1000 Genomes samples (CEU,
202 GBR, FIN, IBS, and TSI). To compute the polygenic risk scores, we considered all
203 SNPs with p-values ≤ 1e-2 in the GWAS study, a window size of 250 kb, and an R^2

threshold of 0.5 in Europeans to group SNPs. After obtaining the top clumped signals, we computed scores using the --score flag in plink.

Polygenic risk score simulations

We simulated genotypes in a coalescent framework with msprime v0.4.0[60] for chromosome 20 incorporating a recombination map of GRCh37 and an assumed mutation rate of 2e-8 mutations / (base pair * generation). We used a demographic model previously inferred using 1000 Genomes sequencing data[13] to simulate individuals that reflect European, East Asian, and African population histories. We focus on these populations as the demography has previously been modeled and this avoids the challenges of simulating the geographically heterogeneous[52] and sex-biased process of admixture in the Americas[61]. To imitate a GWAS with European sample bias and evaluate polygenic risk scores in other populations, we simulated 200,000 European individuals, 200,000 East Asian, and 200,000 African individuals. Next, we assigned "true" causal effect sizes to *m* evenly spaced alleles. Specifically, we randomly assigned effect sizes as:

$$\beta \sim N(0, \frac{h^2}{m})$$

where the normal distribution is specified by the mean and standard deviation (as in python's numpy package). For all other non-causal sites, the effect size is zero. We then define *X* as:

$$X = \sum_{i=1}^{m} g_i \beta_i$$

where the g_i are the genotype states (i.e. 0, 1, or 2). To handle varying allele frequencies, potential weak LD between causal sites, ensure a neutral model with random true polygenic risks with respect to allele frequencies, and to obtain the total desired variance, we normalize *X* as:

$$Z_X = \frac{X - \mu_X}{\sigma_X}$$

We then compute the true polygenic risk score, as:

$$G = \sqrt{h^2} * Z_X$$

such that the total variance of the scores is h^2. We also simulated environmental noise and standardize to ensure equal variance between normalized genetic and environmental effects before, defining the environmental effect *E* as:

$$\begin{aligned} \epsilon =& N(0, 1 - h^2) \\ Z_\epsilon =& \frac{\epsilon - \mu_\epsilon}{\sigma_\epsilon} \\ E =& \sqrt{1 - h^2} * Z_\epsilon \end{aligned}$$

such that the total variance of the environmental effect is $1 - h^2$. We then define the total liability as:

$$\begin{aligned} L =& \sqrt{h^2} * Z_X + \sqrt{1 - h^2} * Z_\epsilon \\ =& G + E \end{aligned}$$

We assigned 10,000 European individuals at the most extreme end of the liability threshold “case” status assuming a prevalence of 5%. We randomly assigned 10,000 different European individuals “control” status. We ran a GWAS with these 10,000 European cases and 10,000 European controls, computing Fisher’s exact test for all

243 sites with MAF > 0.01. As before for empirical polygenic risk score calculations from real
244 GWAS summary statistics, we clumped these SNPs into LD blocks for all sites with p ≤
245 1e-2, $R^2 \geq 0.5$ in Europeans, and within a window size of 250 kb. We used these SNPs
246 to compute inferred polygenic risk scores as before, summing the product of the log
247 odds ratio and genotype for the true polygenic risk in a cohort of 10,000 simulated
248 European, African, and East Asian individuals (all not included in the simulated GWAS).
249 We compared the true versus inferred polygenic risk scores for these individuals across
250 varying complexities (m = 200, 500, 1000) and heritabilites (h^2 = 0.33, 0.50, 0.67).
251

252 **Results**

253 *Genetic diversity within and between populations in the Americas*

254 We first assessed the overall diversity at the global and sub-continental level of the
255 1000 Genomes Project (phase 3) populations[18] using a likelihood model via
256 ADMIXTURE[62] and PCA[63] (**Figure S1** and **Figure S2**). The six populations from the
257 Americas demonstrate considerable continental admixture, with genetic ancestry
258 primarily from Europe, Africa, and the Americas, recapitulating previously observed
259 population structure[18]. To quantify continental genetic diversity in these populations, we
260 repeated the analysis using YRI, CEU, and NAT samples[54] as reference panels
261 (population labels and abbreviations in **Table S1**). We observed widely varying
262 continental admixture contributions in the six populations from the Americas at K=3
263 (**Figure 1**A and **Table S2**). For example, when compared to the ASW, the ACB have a
264 higher proportion of African ancestry (μ = 0.88, 95% CI = [0.87-0.89] versus μ = 0.76,
265 95% CI = [0.73-0.78]; two-sided t-test p=3.0e-13) and a smaller proportion of EUR and

266 NAT ancestry. The PEL have more NAT ancestry than all of the other AMR populations
267 (μ = 0.77, 95% CI = [0.75-0.80] versus CLM: μ = 0.26, 95% CI = [0.24, 0.27], p=2.9e-95;
268 PUR: μ = 0.13, 95% CI = [0.12, 0.13], p=4.8e-93; and MXL: μ = 0.47, 95% CI = [0.43,
269 0.50], p=1.7e-28) ascertained in 1000 Genomes.
270
271 We explored the origin of the subcontinental-level ancestry from recently admixed
272 individuals by identifying local ancestry tracts[29,35,56,64] (Methods, **Figure S3**). As proxy
273 source populations for the recent admixture, we used EUR and AFR continental
274 samples from the 1000 Genomes Project as well as NAT samples genotyped
275 previously[54]. Concordance between global ancestry estimates inferred using
276 ADMIXTURE at K=5 and RFMix was typically high (Pearson's correlation ≥ 98%, see
277 **Figure S4**). Using *Tracts*[57], we modeled the length distribution of the AFR, EUR, and
278 NAT tracts to infer that admixing began ~12 and ~8 generations ago in the PEL and
279 ACB populations, respectively (**Figure S5)**, consistent with previous estimates from
280 other populations from the Americas[49,57,65].
281
282 We further investigated the subcontinental ancestry of admixed populations from the
283 Americas one ancestry at a time using a version of PCA modified to handle highly
284 masked data (ancestry-specific or AS-PCA) as implemented in PCAmask[66]. Example
285 ancestry tracts in a PEL individual subset to AFR, EUR, and NAT components are
286 shown in **Figure 1**B, D, and F, respectively. Consistent with previous observations, the
287 inferred European tracts in Hispanic/Latino populations most closely resemble southern
288 European IBS and TSI populations with some additional drift[35] (**Figure 1**E). The

289 European tracts of the PUR are more differentiated compared to the CLM, MXL, and
290 PEL populations, consistent with sex bias (**Figure S6 and Table S3**) and excess drift
291 from founder effects in this island population[35]. In contrast to the southern European
292 tracts from the Hispanic/Latino populations, the African descent populations in the
293 Americas have European admixture that more closely resembles the northwestern CEU
294 and GBR European populations. The clusters are less distinct, owing to lower overall
295 fractions of European ancestry, however the European components of the
296 Hispanic/Latino and African American populations are significantly different (Wilcoxan
297 rank sum test p=2.4e-60).
298
299 The ability to localize aggregated ancestral genomic tracts enables insights into the
300 evolutionary origins of admixed populations. To disentangle whether the considerable
301 Native American ancestry in the ASW individuals arose from recent admixture with
302 Hispanic/Latino individuals or recent admixture with indigenous Native American
303 populations, we queried the European tracts. We find that the European tracts of all
304 ASW individuals with considerable Native American ancestry are well within the ASW
305 cluster and project closer in Euclidean distance with AS-PC1 and AS-PC2 to
306 northwestern Europe than the European tracts from Hispanic/Latino samples (p=1.15e-
307 3), providing support for the latter hypothesis and providing regional nuance to previous
308 findings[49].
309
310 We also investigated the African origin of the admixed AFR/AMR populations (ACB and
311 ASW), as well as the Native American origin of the Hispanic/Latino populations (CLM,

312 MXL, PEL, and PUR). The African tracts of ancestry from the AFR/AMR populations
313 project closer to the YRI and ESN of Nigeria than the GWD, MSL, and LWK populations
314 (**Figure 1**C). This is consistent with slave records and previous genome-wide analyses
315 of African Americans indicating that most sharing occurred in West and West-Central
316 Africa[67-69]. There are subtle differences between the African origins of the ACB and
317 ASW populations (e.g. difference in distance from YRI on AS-PC1 and AS-PC2 p=6.4e-
318 6), likely due either to mild island founder effects in the ACB samples or differences in
319 African source populations for enslaved Africans who remained in Barbados versus
320 those who were brought to the US. The Native tracts of ancestry from the AMR
321 populations first separate the southernmost PEL populations from the CLM, MXL, and
322 PUR on AS-PC1, then separate the northernmost MXL from the CLM and PUR on AS-
323 PC2, consistent with a north-south cline of divergence among indigenous Native
324 American ancestry (**Figure 1**G). [35,70]
325
326 *Impact of continental and sub-continental diversity on disease variant mapping*
327 To investigate the role of ancestry in phenotype interpretation from genetic data, we
328 assessed diversity across populations and local ancestries for recently admixed
329 populations across the whole genome and sites from two reference databases: the
330 GWAS catalog and ClinVar pathogenic and likely pathogenic sites. We recapitulate
331 results showing that there is less variation across the genome (both genome-wide and
332 on the Affymetrix 6.0 GWAS array sites used in local ancestry calling) in out-of-Africa
333 versus African populations, but that GWAS variants are more polymorphic in European
334 and Hispanic/Latino populations (**Figure S7A-B, Figure S8**A-B). We use a normalized

335 measure of the minor allele frequency, an indicator of the amount of diversity captured
336 in a population, to obtain a background coverage of each population, as done previously
337 (e.g. Figure S4 from phase 3 of the 1000 Genomes Project[18]). We show that the
338 Affymetrix 6.0 array has a slight European bias (**Figure S5**A and **Figure S6**A). We
339 compared the site frequency spectrum of variants across the genome versus at GWAS
340 catalog sites, and identify elevated allele frequencies at GWAS catalog loci, particularly
341 in populations with more European ancestry (e.g. the EUR, AMR, and SAS super
342 populations, **Figure S5**C-D). We further compared heterozygosity (estimated here as
343 *2pq*) and the site frequency spectrum in recently admixed populations across diploid
344 and haploid local ancestry tracts, respectively. Sites in the GWAS catalog and ClinVar
345 are more and less common than genome-wide variants, respectively (**Figure 2**).
346 Whereas heterozygosity across the whole genome is highest in African ancestry tracts,
347 it is consistently the greatest in European ancestry tracts across these databases
348 (**Figure 2** and **Figure S8**C-D), reflecting a strong bias towards European study
349 participants[1-4,18,71]. These results highlight imbalances in genome interpretability across
350 local ancestry tracts in recently admixed populations and the utility of analyzing these
351 variants jointly with these ancestry tracts over genome-wide ancestry estimates alone.
352
353 We also assessed imputation accuracy across the 3-way admixed populations from the
354 Americas (CLM, MXL, PEL, PUR) for two arrays: the Illumina OmniExpress and the
355 Affymetrix Axiom World Array LAT. Imputation accuracy was estimated as the
356 correlation (r^2) between the original genotypes and the imputed dosages. For both array
357 designs, imputation accuracy across all minor allele frequency (MAF) bins was highest

358 for populations with the largest proportion of European ancestry (PUR) and lowest for
359 populations with the largest proportion of Native American ancestry (PEL, **Figure S9**A-
360 B). We also stratified imputation accuracy by local ancestry tract diplotype within the
361 Americas. Consistently, tracts with at least one Native American ancestry tract had
362 lower imputation accuracy when compared to tracts with only European and/or African
363 ancestry (**Figure 3** and **Figure S10**).
364
365 *Transferability of GWAS findings across populations*
366 To quantify the transferability of European-biased genetic studies to other populations,
367 we next used published GWAS summary statistics to infer polygenic risk scores[72]
368 across populations for well-studied traits, including height[9], waist-hip ratio[73],
369 schizophrenia[10], type II diabetes[74,75], and asthma[76] (**Figure 4**A-D, **Figure S11**,
370 Methods). Most of these summary statistics are derived from studies with primarily
371 European cohorts, although GWAS of type II diabetes have been performed in both
372 European-specific cohorts as well as across multi-ethnic cohorts. We identify clear
373 directional inconsistencies in these score inferences. For example, although the height
374 summary statistics show the expected cline of southern/northern cline of increasing
375 European height (FIN, CEU, and GBR populations have significantly higher polygenic
376 risk scores than IBS and TSI, p=1.5e-75, **Figure S9**A), polygenic scores for height
377 across super populations show biased predictions. For example, the African populations
378 sampled are genetically predicted to be considerably shorter than all Europeans and
379 minimally taller than East Asians (**Figure 4**A), which contradicts empirical observations
380 (with the exception of some indigenous pygmy/pygmoid populations)[77,78]. Additionally,

381 polygenic risk scores for schizophrenia, while at a similar prevalence across populations
382 where it has been well-studied[79] and sharing significant genetic risk across
383 populations[80], shows considerably decreased scores in Africans compared to all other
384 populations (**Figure 4**B). Lastly, the relative order of polygenic risk scores computed for
385 type II diabetes across populations differs depending on whether the summary statistics
386 are derived from a European-specific (**Figure 4**C) or multi-ethnic (**Figure 4**D) cohort.
387
388 *Ancestry-specific biases in polygenic risk score estimates*
389 We performed coalescent simulations to determine how GWAS signals discovered in
390 one ancestral case/control cohort (i.e. 'single-ancestry' GWAS) are expected to impact
391 polygenic risk score estimates in other populations under neutrality using summary
392 statistics (for details, see Methods). Briefly, we simulated variants according to a
393 previously published demographic model inferred from Africans, East Asians, and
394 Europeans[13]. We specified "causal" alleles and effect sizes randomly, such that each
395 causal variant has evolved neutrally and has a mean effect of zero with the standard
396 deviation equal to the global heritability divided by number of causal variants. We then
397 computed the true polygenic risk for each individual as the product of the estimated
398 effect sizes and genotypes, then standardized the scores across all individuals. We
399 calculated the total liability as the sum of the genetic and random environmental
400 contributions, then identified 10,000 European cases with the most extreme liabilities
401 and 10,000 other European controls. We then computed Fisher's exact tests with this
402 European case-control cohort, then quantified inferred polygenic risk scores as the sum

403 of the product of genotypes and log odds ratios for 10,000 samples per population not
404 included in the GWAS.
405
406 In our simulations and consistent with realistic coalescent models, most variants are
407 rare and population-specific; “causal” variants are sampled from the global site
408 frequency spectrum, resulting in subtle differences in true polygenic risk across
409 populations (**Figure S12, Figure 5**B-D). We mirrored standard practices for performing
410 a GWAS and computing polygenic risk scores (see above and Methods). We find that
411 the correlation between true and inferred polygenic risk is generally low (**Figure 5**A,
412 **Figure S13**), consistent with limited variance explained by polygenic risk scores from
413 GWAS of these cohort sizes for height (e.g. ~10% of variance explained for a cohort of
414 size 183,727[81]) and schizophrenia (e.g. ~7% variance explained for a cohort of size
415 36,989 cases and 113,075 controls[10]). Low correlations in our simulations are most
416 likely because common tag variants are a poor proxy for rare causal variants. As
417 expected, correlations between true and inferred risk within populations are typically
418 highest in the European population (i.e. the population in which variants were
419 discovered, **Figure 5**A and **Figure S13**). Across all populations, the mean Spearman
420 correlations between true and inferred polygenic risk increase with increasing heritability
421 while the standard deviation of these correlations significantly decreases ($p=0.05$);
422 however, there is considerable within-population heterogeneity resulting in high
423 variation in scores across all populations. We find that in these neutral simulations, a
424 polygenic risk score bias in essentially any direction is possible even when choosing the
425 exact same causal variants, heritability, and varying only fixed effect size (i.e. inferred

426 polygenic risk in Europeans can be higher, lower, or intermediate compared to true risk
427 relative to East Asians or Africans, **Figure S12, Figure 5**B-D).
428
429 While causal variants in our simulations are drawn from the global site frequency
430 spectrum and are therefore mostly rare, inferred scores are derived specifically from
431 common variants that are typically much more common in the study population than
432 elsewhere (here Europeans with case/control MAF ≥ 0.01). Consequently, the
433 distribution of mean true polygenic risk across simulation runs for each population are
434 not significantly different (**Figure 5**E); however, inferred risk is considerably less than
435 zero in Europeans (p=1.9e-54, 95% CI=[-84.3, -67.4]), slightly less than zero in East
436 Asians (p=5.9e-5, 95% CI=[-19.1, -6.6]) and not significantly different from zero in
437 Africans, with variance in risk scores decreasing with this trend (**Figure 5**F). The scale
438 is orders of magnitude different between the true and inferred unstandardized scores,
439 cautioning that while they are informative on a relative scale (**Figure 5**A and **Figure**
440 **S11**), their absolute scale should not be overinterpreted. The inferred risk difference
441 between populations is driven by the increased power to detect minor risk alleles rather
442 than protective alleles in the study population[82], given the differential selection of cases
443 and controls in the liability threshold model. We demonstrate this empirically in these
444 neutral simulations within the European population (**Figure 5**G), indicating that this
445 phenomenon occurs even in the absence of population structure and when case and
446 control cohort sizes are equal.
447
448 **Discussion**

449 To date, GWAS have been performed opportunistically in primarily single-ancestry
450 European cohorts, and an open question remains about their biomedical relevance for
451 disease associations in other ancestries. As studies gain power by increasing sample
452 sizes, effect size estimates become more precise and novel associations at lower
453 frequencies are feasible. However, rare variants are largely population-private, and their
454 effects are unlikely to transfer to new populations. Because linkage disequilibrium and
455 allele frequencies vary across ancestries, effect size estimates from diverse cohorts are
456 typically more precise than from single-ancestry cohorts (and often tempered)[5], and the
457 resolution of causal variant fine-mapping is considerably improved[75]. Across a range of
458 genetic architectures, diverse cohorts provide the opportunity to reduce false positives.
459 At the Mendelian end of the spectrum, for example, disentangling risk variants with
460 incomplete penetrance from benign false positives and localizing functional effects in
461 genes is much more feasible with large diverse population cohorts than possible with
462 single-ancestry analyses[83,84]. Multiple false positive reports of pathogenic variants
463 causing hypertrophic cardiomyopathy, a disease with relatively simple genomic
464 architecture, have been returned to patients of African descent or unspecified ancestry
465 that would have been prevented if even a small number of African American samples
466 were included in control cohorts[85]. At the highly complex end of the polygenicity
467 spectrum, we and others have shown that the utility of polygenic risk inferences and the
468 heritable phenotypic variance explained in diverse populations is improved with more
469 diverse cohorts[80,86].
470

471 Standard single-ancestry GWAS typically apply linear mixed model approaches and/or
472 incorporate principal components as covariates to control for confounding from
473 population structure with primarily European-descent cohorts[1-3]. A key concern when
474 including multiple diverse populations in a GWAS is that there is increasing likelihood of
475 identifying false positive variants associated with disease that are driven by allele
476 frequency differences across ancestries. However, previous studies have analyzed
477 association data for diverse ancestries and replicated findings across ethnicities,
478 assuaging these concerns[7,75,87]. In this study, we show that this ancestry stratification is
479 not continuous along the genome: long tracts of ancestrally diverse populations present
480 in admixed samples from the Americas are easily and accurately detected. Querying
481 population substructure within these tracts recapitulates expected trends, e.g. European
482 ancestry in African Americans primarily descends from northern Europeans in contrast
483 to European ancestry from Hispanic/Latinos, which primarily descends from southern
484 Europeans, as seen previously[49]. Additionally, population substructure follows a north-
485 south cline in the Native component of Hispanic/Latinos, and the African component of
486 admixed African descent populations in the Americas most closely resembles reference
487 populations from Nigeria (albeit given the limited set of African populations from The
488 1000 Genomes Project). Admixture mapping has been successful at large sample sizes
489 for identifying ancestry-specific genetic risk factors for disease[88]. Given the level of
490 accuracy and subcontinental-resolution attained with local ancestry tracts in admixed
491 populations, we emphasize the utility of a unified framework to jointly analyze genetic
492 associations with local ancestry simultaneously[45].
493

494 The transferability of GWAS is aided by the inclusion of diverse populations[89]. We have
495 shown that European discovery biases in GWAS are recapitulated in local ancestry
496 tracts in admixed samples. We have quantified GWAS study biases in ancestral
497 populations and shown that GWAS variants are at lower frequency specifically within
498 African and Native tracts and higher frequency in European tracts in admixed American
499 populations. Imputation accuracy is also stratified across diverged ancestries, including
500 across local ancestries in admixed populations. With decreased imputation accuracy
501 especially on Native American tracts, there is decreased power for potential ancestry-
502 specific associations. This differentially limits conclusions for GWAS in an admixed
503 population in a two-pronged manner: the ability to capture variation and the power to
504 estimate associations.
505
506 As GWAS scale to sample sizes on the order of hundreds of thousands to millions,
507 genetic risk prediction accuracy at the individual level improves[90]. However, we show
508 that the utility of polygenic risk scores computed using GWAS summary statistics are
509 dependent on genetic similarity to the discovery cohort. BLUP risk prediction methods
510 have been proposed to improve risk scores, but they require access to raw genetic data
511 typically from very large datasets, are also dependent on LD structure in the study
512 population, and only offer modest improvements in prediction accuracy[91]. Furthermore,
513 polygenic risk scores contain a mix of true positives (which have the bias described
514 above) and false positives in the training GWAS. False positives, being chance
515 statistical fluctuations, do not have the same allele frequency bias and therefore
516 unfortunately play an outsized role in applying a PRS in a new population.

We have demonstrated that polygenic risk computed from summary statistics in a single-ancestry cohort can be biased in essentially any direction across diverse populations simply as a result of genetic drift, limiting their interpretability; directional selection is expected to bias polygenic risk inferences even more. Because biases arise from genetic drift alone, we recommend: 1) avoiding interpretations from polygenic risk score differences extrapolated across populations, as these are likely confounded by latent population structure that is not properly corrected for with current methods, 2) mean-centering polygenic risk scores for each population, and 3) computing polygenic risk scores in populations with similar demographic histories as the study sample to ensure maximal predictive power. Further, additional methods that account for local ancestry in genetic risk prediction to incorporate different ancestral linkage disequilibrium and allele frequencies are needed. This study demonstrates the utility of disentangling ancestry tracts in recently admixed populations for inferring recent demographic history and identifying ancestry-stratified analytical biases; we also motivate the need to include more ancestrally diverse cohorts in GWAS to ensure that health disparities arising from genetic risk prediction do not become pervasive in individuals of admixed and non-European descent.

Competing interests

CDB is an SAB member of Liberty Biosecurity, Personalis, Inc., 23andMe Roots into the Future, Ancestry.com, IdentifyGenomics, LLC, Etalon, Inc., and is a founder of CDB

539 Consulting, LTD. CRG owns stock in 23andMe, Inc. All other authors declare that they
540 have no competing interests.
541
542 **Author contributions**
543 ARM, CRG, RKW, CDB, MJD, EEK conceived of and designed the experiments. ARM
544 and GLW performed the data analysis. SG, CDB, and MJD contributed analysis
545 tools/materials. ARM wrote the manuscript with comments from CRG, RKW, GLW,
546 MJD, SG, and EEK. All authors read and approved the final manuscript.
547
548 **Acknowledgments**
549 We thank Suyash Shringarpure, Brian Maples, Andres Moreno-Estrada, Danny Park,
550 Noah Zaitlen, Alexander Gusev, and Alkes Price for helpful discussions/feedback. We
551 thank Verneri Antilla for providing GWAS summary statistics. We thank Jerome Kelleher
552 for several conversations about msprime, providing example scripts, and implementing
553 new simulation capabilities. This work was supported by funds from several grants; the
554 National Human Genome Research Institute under award numbers U01HG009080
555 (EEK, CDB, CRG), U01HG007419 (CDB, CRG, GLW), U01HG007417 (EEK),
556 U01HG005208 (MJD), T32HG000044 (CRG) and R01GM083606 (CDB), and the
557 National Institute of General Medical Sciences under award number T32GM007790
558 (ARM) at the National Institute of Health; the Directorate of Mathematical and Physical
559 Sciences award 1201234 (SG, CDB) at the National Science Foundation; the Canadian
560 Institutes of Health Research through the Canada Research Chair program and
561 operating grant MOP-136855 (SG), and a Sloan Research Fellowship (SG).

562

563 **Web Resources**

564 Phased 1000 Genomes haplotypes: ftp://ftp-

565 trace.ncbi.nih.gov/1000genomes/ftp/release/20130502/supporting/shapeit2_scaffolds/w

566 gs_gt_scaffolds/

567 Local ancestry calls: https://personal.broadinstitute.org/armartin/tgp_admixture/

568 Scripts for processing data and running simulations:

569 https://github.com/armartin/ancestry_pipeline/

570 PCAmask software: https://sites.google.com/site/pcamask/dowload

571 Tracts software: https://github.com/sgravel/tracts

572 Msprime software: https://github.com/jeromekelleher/msprime

573

574 **Figure captions**

575

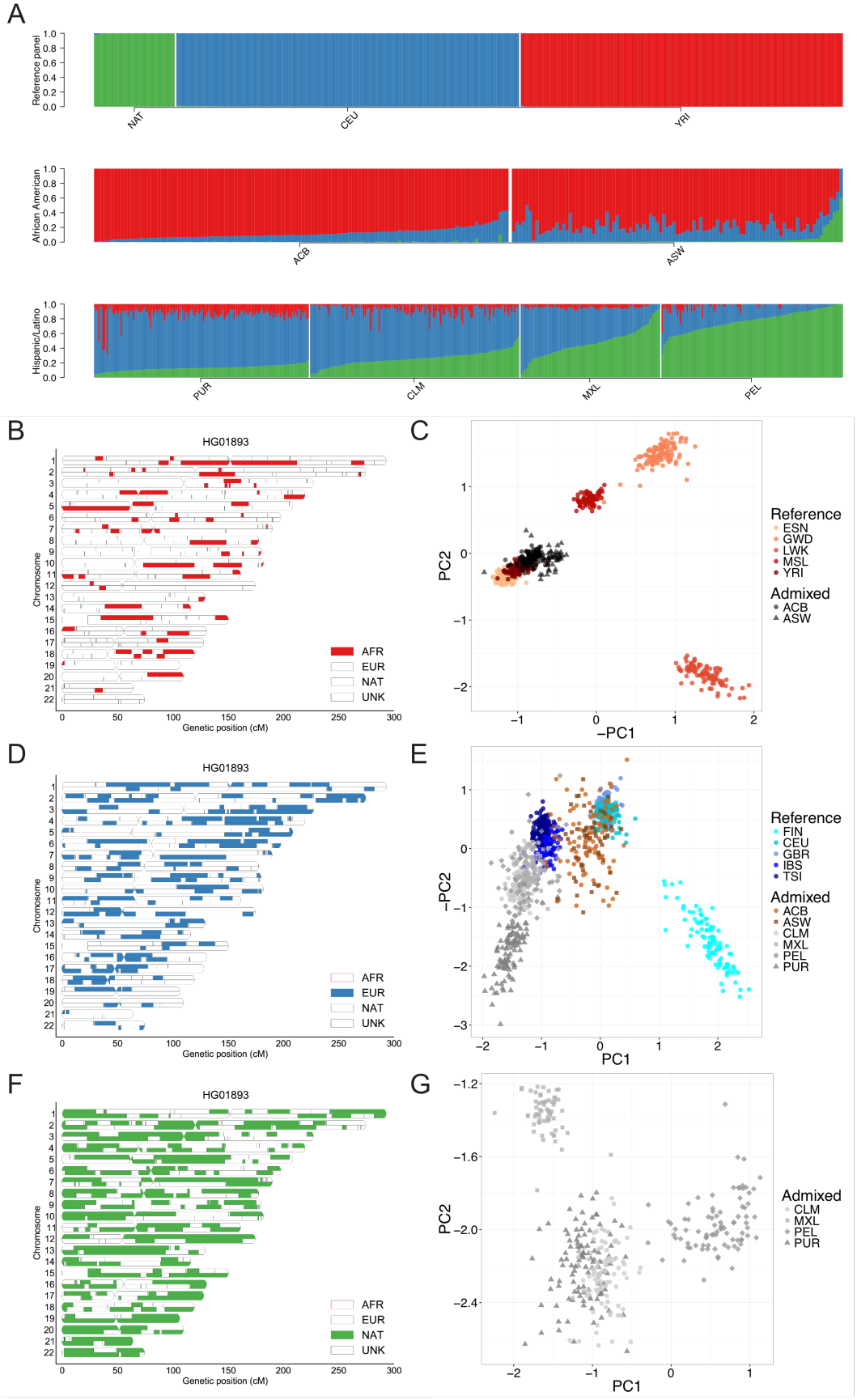
A
Reference panel
NAT
CEU
YRI
African American
ACB
ASW
Hispanic/Latino
PUR
CLM
MXL
PEL
B
HG01893
Chromosome
Genetic position (cM)
AFR
EUR
NAT
UNK
C
PC2
−PC1
Reference
ESN
GWD
LWK
MSL
YRI
Admixed
ACB
ASW
D
HG01893
Chromosome
Genetic position (cM)
AFR
EUR
NAT
UNK
E
−PC2
PC1
Reference
FIN
CEU
GBR
IBS
TSI
Admixed
ACB
ASW
CLM
MXL
PEL
PUR
F
HG01893
Chromosome
Genetic position (cM)
AFR
EUR
NAT
UNK
G
PC2
PC1
Admixed
CLM
MXL
PEL
PUR

576

577 **Figure 1** – Sub-continental diversity and origins of African, European, and Native
578 American components of recently admixed Americas populations. A) ADMIXTURE
579 analysis at K=3 focusing on admixed Americas samples, with the NAT[54], CEU, and YRI
580 as reference populations. B,D,F) Local ancestry karyograms for representative PEL
581 individual HG01893 with B) African, D) European, and F) Native American components
582 shown. C,E,G) Ancestry-specific PCA applied to admixed haploid genomes as well as
583 ancestrally homogeneous continental reference populations from 1000 Genomes
584 (where possible) for C) African tracts, E) European tracts, and G) Native American
585 tracts. A small number of admixed samples that constituted major outliers from the
586 ancestry-specific PCA analysis were removed, including C) 1 ASW sample (NA20314)
587 and E) 8 samples, including 3 ACB, 2 ASW, 1 PEL, and 2 PUR samples.

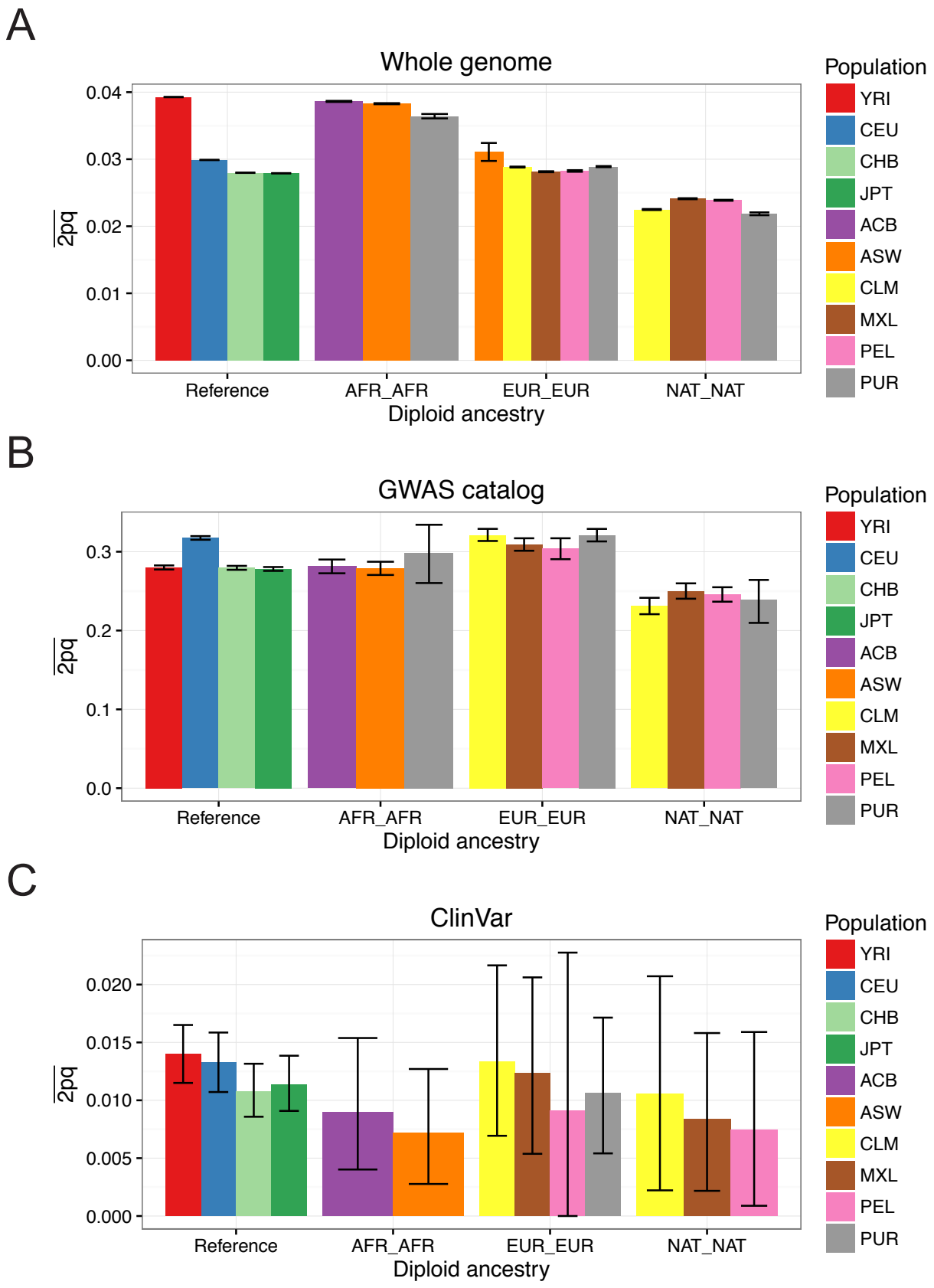
A
Whole genome
0.04
0.03
0.02
0.01
0.00
2pq
Reference
AFR_AFR
EUR_EUR
NAT_NAT
Diploid ancestry
Population
YRI
CEU
CHB
JPT
ACB
ASW
CLM
MXL
PEL
PUR
B
GWAS catalog
0.3
0.2
0.1
0.0
2pq
Reference
AFR_AFR
EUR_EUR
NAT_NAT
Diploid ancestry
Population
YRI
CEU
CHB
JPT
ACB
ASW
CLM
MXL
PEL
PUR
C
ClinVar
0.020
0.015
0.010
0.005
0.000
2pq
Reference
AFR_AFR
EUR_EUR
NAT_NAT
Diploid ancestry
Population
YRI
CEU
CHB
JPT
ACB
ASW
CLM
MXL
PEL
PUR

588

589 **Figure 2** – Heterozygosity (estimated here as 2pq) in admixed populations stratified by
590 diploid local ancestry in A) the whole genome, B) sites from the GWAS catalog, and C)
591 sites from ClinVar classified as “pathogenic” or “likely pathogenic.” The mean and 95%
592 confidence intervals were calculatated by bootstrapping 1000 times. Populations not
593 shown in a given panel have too few diploid ancestry tracts overlapping sites to
594 calculate heterozygosity.
595

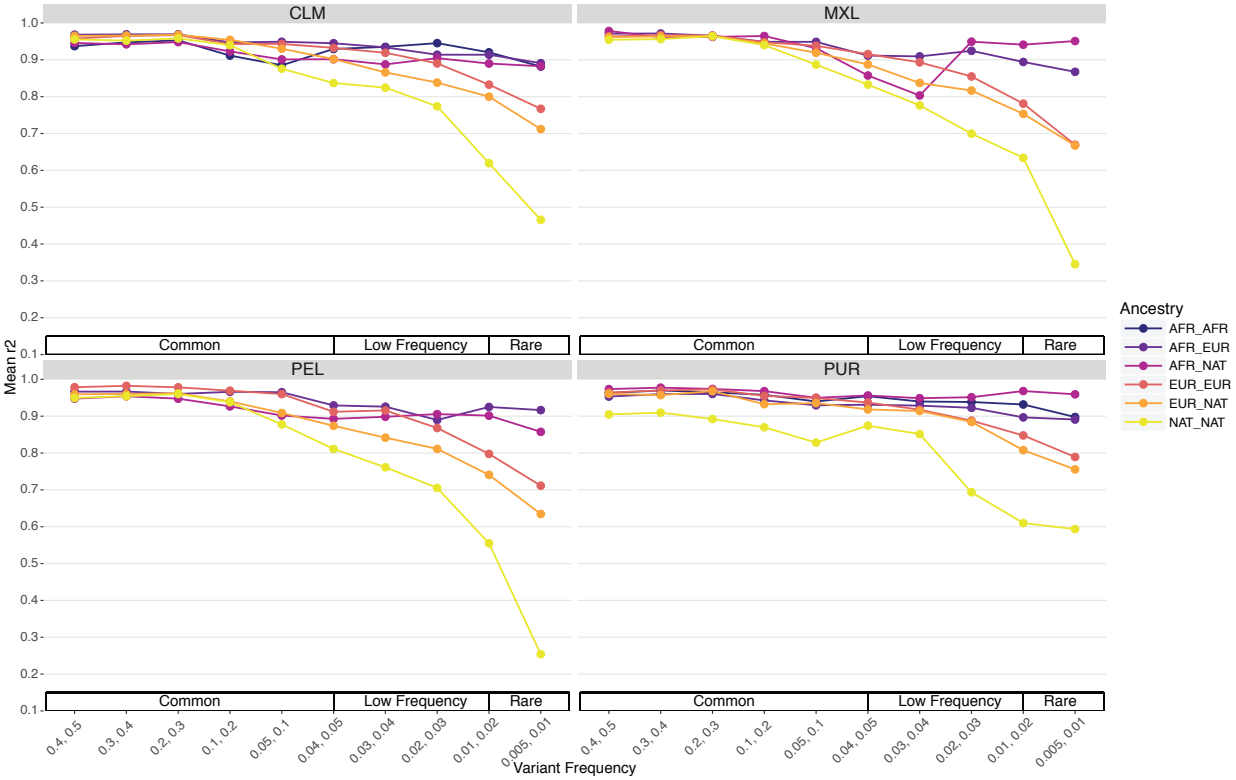

596

597 **Figure 3** - Imputation accuracy by population assessed using a leave-on-out strategy,
598 stratified by diploid local ancestry on chromosome 9 for the Illumina OmniExpress
599 genotyping array.

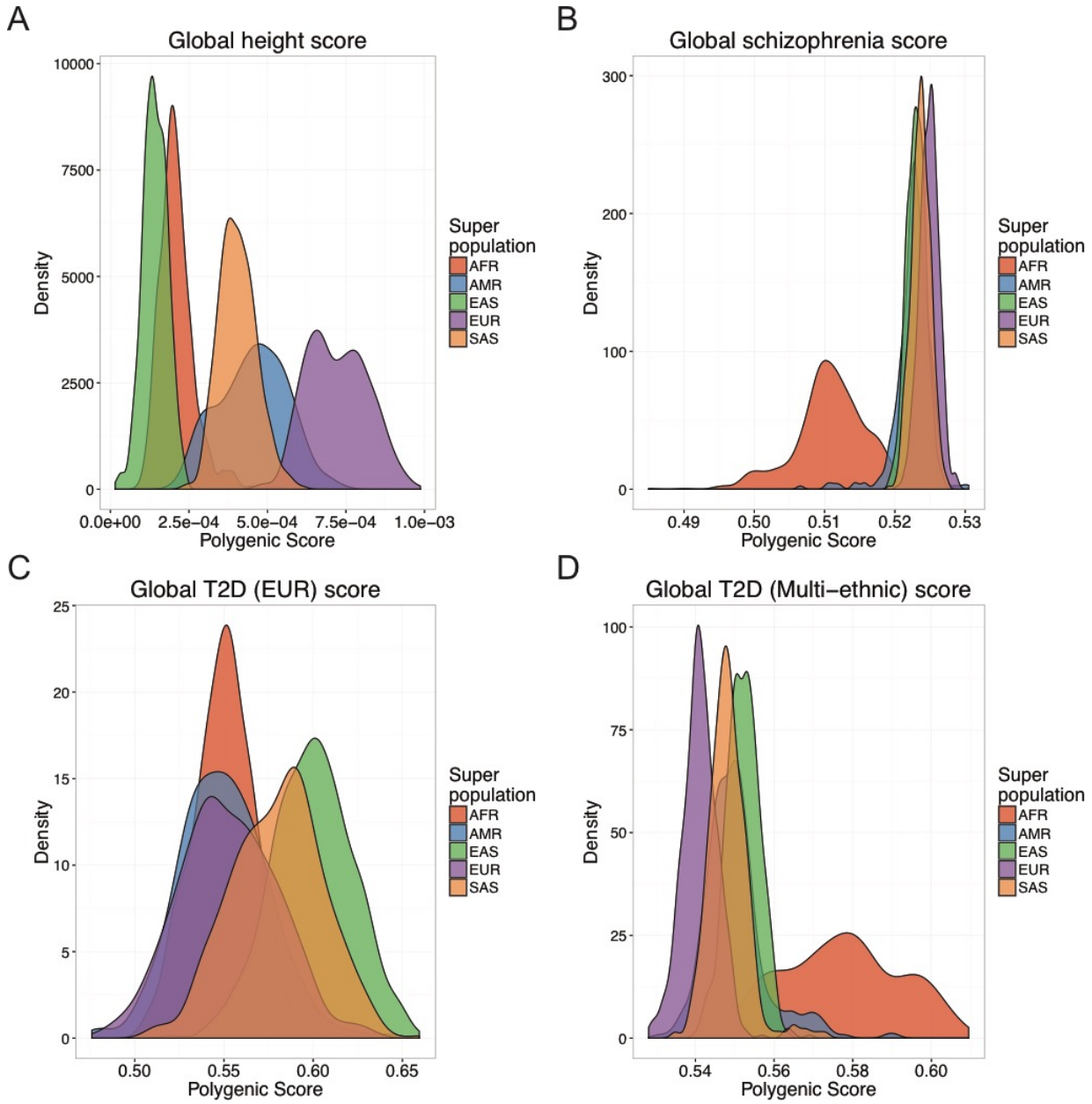

Figure 4 - Biased genetic discoveries influence disease risk inferences. A-D) Inferred polygenic risk scores across individuals colored by population for: A) height based on summary statistics from [9]. B) schizophrenia based on summary statistics from [10]. C) type II diabetes summary statistics derived from a European cohort from [74]. D) type II diabetes summary statistics derived from a multiethnic cohort from [75].

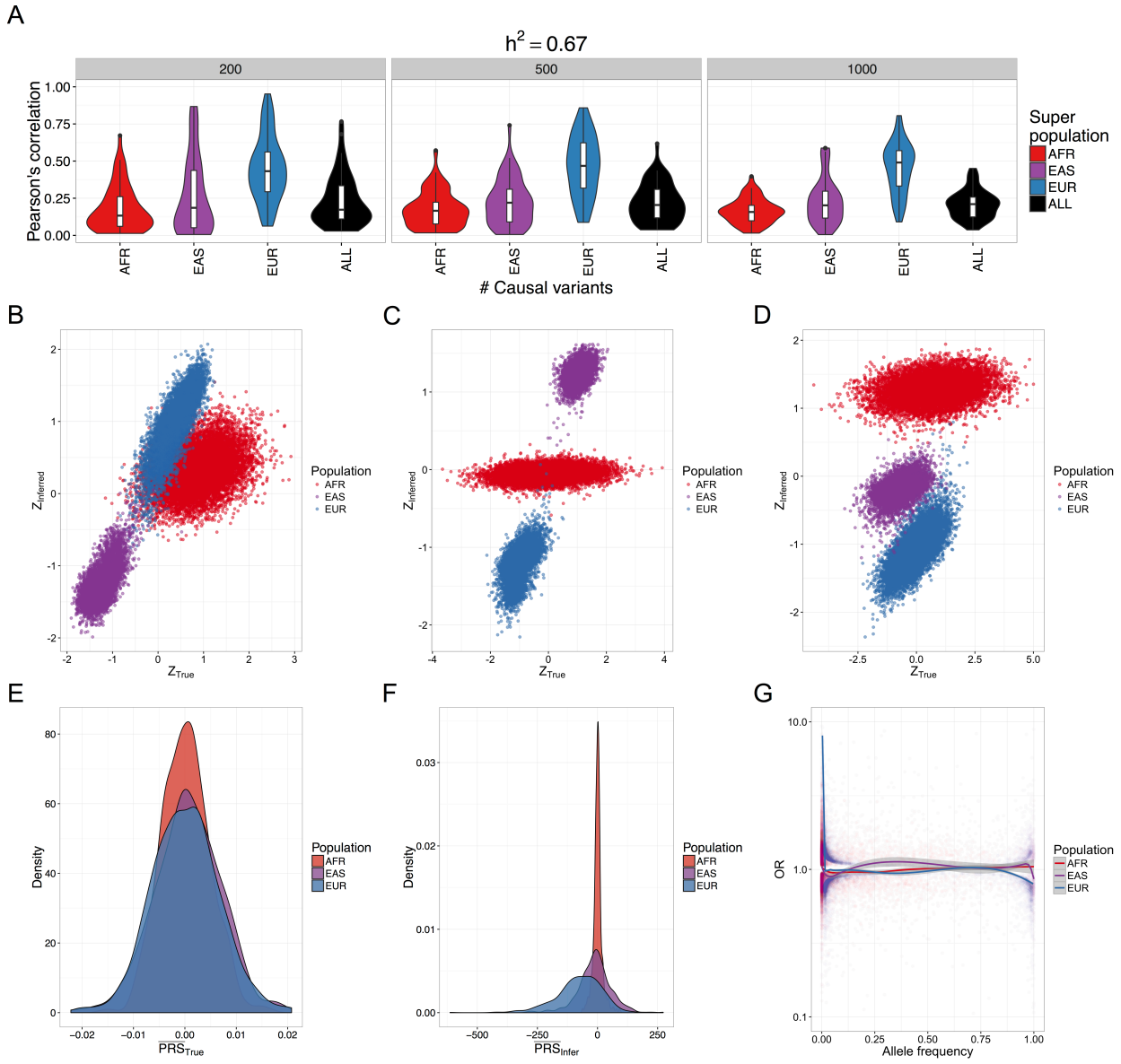

Figure 5 - Coalescent simulation results for true vs inferred polygenic risk scores computed from GWAS summary statistics with 10,000 cases and 10,000 controls modeling European, East Asian, and African population history (demographic parameters from [13]). A) Violin plots show Pearson's correlation across 50 iterations per parameter set between true and inferred polygenic risk scores across differing genetic architectures, including *m*=200, 500, and 1,000 causal variants and h^2=0.67. The "ALL" population correlations were performed on population mean-centered true and inferred polygenic risk scores. B-D) Standardized true versus inferred polygenic risk scores for 3

615 different coalescent simulations showing 10,000 randomly drawn samples from each
616 population not included as cases or controls. E-F) The distribution for each population
617 across 500 simulations with *m*=1000 causal variants and h^2=0.67 of: E) unstandardized
618 mean true polygenic risk and F) unstandardized mean inferred polygenic risk. G) Allele
619 frequency versus inferred odds ratio for sites included in inferred polygenic risk scores
620 for each population across 500 simulations, as in E-F).
621

622 **References**

623 1. Need AC, Goldstein DB (2009) Next generation disparities in human genomics:
624 concerns and remedies. Trends in genetics : TIG 25:489-494
625 2. Bustamante CD, Francisco M, Burchard EG (2011) Genomics for the world. Nature
626 475:163-165
627 3. Petrovski S, Goldstein DB (2016) Unequal representation of genetic variation across
628 ancestry groups creates healthcare inequality in the application of precision medicine.
629 Genome Biology 17:157
630 4. Popejoy AB, Fullerton SM (2016) Genomics is failing on diversity. Nature 538:161
631 5. Carlson CS, Matise TC, North KE, Haiman CA, Fesinmeyer MD, Buyske S,
632 Schumacher FR, Peters U, Franceschini N, Ritchie MD, et al (2013) Generalization and
633 dilution of association results from European GWAS in populations of non-European
634 ancestry: the PAGE study. PLoS Biol 11:e1001661
635 6. Torgerson DG, Ampleford EJ, Chiu GY, Gauderman WJ, Gignoux CR, Graves PE,
636 Himes BE, Levin AM, Mathias RA, Hancock DB, et al (2011) Meta-analysis of genome-
637 wide association studies of asthma in ethnically diverse North American populations.
638 Nature genetics 43:887-892
639 7. Waters KM, Stram DO, Hassanein MT, Le Marchand L, Wilkens LR, Maskarinec G,
640 Monroe KR, Kolonel LN, Altshuler D, Henderson BE, et al (2010) Consistent association
641 of type 2 diabetes risk variants found in europeans in diverse racial and ethnic groups.
642 PLoS Genet 6
643 8. Hindorff LA, Sethupathy P, Junkins HA, Ramos EM, Mehta JP, Collins FS, Manolio
644 TA (2009) Potential etiologic and functional implications of genome-wide association

645 loci for human diseases and traits. Proceedings of the National Academy of Sciences
646 106:9362-9367
647 9. Wood AR, Esko T, Yang J, Vedantam S, Pers TH, Gustafsson S, Chu AY, Estrada K,
648 Luan J, Kutalik Z, et al (2014) Defining the role of common variation in the genomic and
649 biological architecture of adult human height. Nature genetics 46:1173-1186
650 10. Schizophrenia Working Group of the Psychiatric Genomics Consortium (2014)
651 Biological insights from 108 schizophrenia-associated genetic loci. Nature 511:421-427
652 11. Muñoz M, Pong-Wong R, Canela-Xandri O, Rawlik K, Haley CS, Tenesa A (2016)
653 Evaluating the contribution of genetics and familial shared environment to common
654 disease using the UK Biobank. Nat Genet
655 12. Mathieson I, McVean G (2012) Differential confounding of rare and common
656 variants in spatially structured populations. Nature Genetics 44:243-246
657 13. Gravel S, Henn BM, Gutenkunst RN, Indap AR, Marth GT, Clark AG, Yu F, Gibbs
658 RA, Bustamante CD (2011) Demographic history and rare allele sharing among human
659 populations. Proceedings of the National Academy of Sciences of the United States of
660 America 108:11983-11988
661 14. Walter K, Min JL, Huang J, Crooks L, Memari Y, McCarthy S, Perry JRB, Xu C,
662 Futema M, Lawson D, et al (2015) The UK10K project identifies rare variants in health
663 and disease. Nature
664 15. Novembre J, Johnson T, Bryc K, Kutalik Z, Boyko AR, Auton A, Indap A, King KS,
665 Bergmann S, Nelson MR, et al (2008) Genes mirror geography within Europe. Nature
666 456:98-101

667 16. Do R, Kathiresan S, Abecasis GR (2012) Exome sequencing and complex disease:
668 Practical aspects of rare variant association studies. Human Molecular Genetics 21:1-9
669 17. Lek M, Karczewski KJ, Minikel EV, Samocha KE, Banks E, Fennell T, O'Donnell-
670 Luria AH, Ware JS, Hill AJ, Cummings BB, et al (2016) Analysis of protein-coding
671 genetic variation in 60,706 humans. Nature 536:285-291
672 18. Auton A, Abecasis GR, Altshuler DM, Durbin RM, Abecasis GR, Bentley DR,
673 Chakravarti A, Clark AG, Donnelly P, Eichler EE, et al (2015) A global reference for
674 human genetic variation. Nature 526:68-74
675 19. Tennessen JA, Bigham AW, O'Connor TD, Fu W, Kenny EE, Gravel S, McGee S,
676 Do R, Liu X, Jun G, et al (2012) Evolution and functional impact of rare coding variation
677 from deep sequencing of human exomes. Science (New York, N.Y.) 337:64-69
678 20. Grossman SR, Shlyakhter I, Karlsson EK, Byrne EH, Morales S, Frieden G,
679 Hostetter E, Angelino E, Garber M, Zuk O, et al (2010) A composite of multiple signals
680 distinguishes causal variants in regions of positive selection. Science (New York, N.Y.)
681 327:883-886
682 21. MacArthur DG, Balasubramanian S, Frankish A, Huang N, Morris J, Walter K,
683 Jostins L, Habegger L, Pickrell JK, Montgomery SB, et al (2012) A systematic survey of
684 loss-of-function variants in human protein-coding genes. Science (New York, N.Y.)
685 335:823-828
686 22. Henn BM, Botigué LR, Peischl S, Dupanloup I, Lipatov M, Maples BK, Martin AR,
687 Musharoff S, Cann H, Snyder MP, et al (2016) Distance from sub-Saharan Africa
688 predicts mutational load in diverse human genomes. Proceedings of the National
689 Academy of Sciences of the United States of America 113:E440-E449

690 23. Lohmueller KE, Indap AR, Schmidt S, Boyko AR, Hernandez RD, Hubisz MJ,
691 Sninsky JJ, White TJ, Sunyaev SR, Nielsen R, et al (2008) Proportionally more
692 deleterious genetic variation in European than in African populations. Nature 451:994-
693 997
694 24. Fu W, Gittelman RM, Bamshad MJ, Akey JM (2014) Characteristics of Neutral and
695 Deleterious Protein-Coding Variation among Individuals and Populations. The American
696 Journal of Human Genetics 95:421-436
697 25. Simons YB, Turchin MC, Pritchard JK, Sella G (2014) The deleterious mutation load
698 is insensitive to recent population history. Nature genetics 46:220-224
699 26. Stokowski RP, Pant PVK, Dadd T, Fereday A, Hinds DA, Jarman C, Filsell W,
700 Ginger RS, Green MR, van der Ouderaa FJ, et al (2007) A genomewide association
701 study of skin pigmentation in a South Asian population. American journal of human
702 genetics 81:1119-1132
703 27. Marcheco-Teruel B, Parra EJ, Fuentes-Smith E, Salas A, Buttenschøn HN,
704 Demontis D, Torres-Español M, Marín-Padrón LC, Gómez-Cabezas EJ, Alvarez-
705 Iglesias V, et al (2014) Cuba: exploring the history of admixture and the genetic basis of
706 pigmentation using autosomal and uniparental markers. PLoS genetics 10:e1004488
707 28. Adhikari K, Fontanil T, Cal S, Mendoza-Revilla J, Fuentes-Guajardo M, Chacón-
708 Duque J, Al-Saadi F, Johansson JA, Quinto-Sanchez M, Acuña-Alonzo V, et al (2016) A
709 genome-wide association scan in admixed Latin Americans identifies loci influencing
710 facial and scalp hair features. Nature Communications 7:10815

711 29. Price AL, Tandon A, Patterson N, Barnes KC, Rafaels N, Ruczinski I, Beaty TH,
712 Mathias R, Reich D, Myers S (2009) Sensitive detection of chromosomal segments of
713 distinct ancestry in admixed populations. PLoS genetics 5:e1000519
714 30. Pasaniuc B, Zaitlen N, Lettre G, Chen GK, Tandon A, Kao WHL, Ruczinski I,
715 Fornage M, Siscovick DS, Zhu X, et al (2011) Enhanced statistical tests for GWAS in
716 admixed populations: Assessment using african americans from CARe and a breast
717 cancer consortium. PLoS Genetics 7
718 31. Fejerman L, Chen GK, Eng C, Huntsman S, Hu D, Williams A, Pasaniuc B, John
719 EM, Via M, Gignoux C, et al (2012) Admixture mapping identifies a locus on 6q25
720 associated with breast cancer risk in US Latinas. Human molecular genetics 21:1907-
721 1917
722 32. Fejerman L, Ahmadiyeh N, Hu D, Huntsman S, Beckman KB, Caswell JL, Tsung K,
723 John EM, Torres-Mejia G, Carvajal-Carmona L, et al (2014) Genome-wide association
724 study of breast cancer in Latinas identifies novel protective variants on 6q25. Nat
725 Commun 5:5260
726 33. Freedman ML, Haiman CA, Patterson N, McDonald GJ, Tandon A, Waliszewska A,
727 Penney K, Steen RG, Ardlie K, John EM, et al (2006) Admixture mapping identifies
728 8q24 as a prostate cancer risk locus in African-American men. Proceedings of the
729 National Academy of Sciences of the United States of America 103:14068-14073
730 34. Bhatia G, Patterson N, Pasaniuc B, Zaitlen N, Genovese G, Pollack S, Mallick S,
731 Myers S, Tandon A, Spencer C, et al (2011) Genome-wide comparison of African-
732 ancestry populations from CARe and other cohorts reveals signals of natural selection.
733 American journal of human genetics 89:368-381

734 35. Moreno-Estrada A, Gravel S, Zakharia F, McCauley JL, Byrnes JK, Gignoux CR,
735 Ortiz-Tello PA, Martínez RJ, Hedges DJ, Morris RW, et al (2013) Reconstructing the
736 Population Genetic History of the Caribbean. PLoS Genetics 9:e1003925
737 36. Bryc K, Velez C, Karafet T, Moreno-Estrada A, Reynolds A, Auton A, Hammer M,
738 Bustamante CD, Ostrer H (2010) Colloquium paper: genome-wide patterns of
739 population structure and admixture among Hispanic/Latino populations. Proceedings of
740 the National Academy of Sciences of the United States of America 107 Suppl :8954-
741 8961
742 37. Pritchard JK, Stephens M, Donnelly P (2000) Inference of population structure using
743 multilocus genotype data. Genetics 155:945-959
744 38. Tang H, Peng J, Wang P, Risch NJ (2005) Estimation of individual admixture:
745 Analytical and study design considerations. Genetic Epidemiology 28:289-301
746 39. Alexander DH, Novembre J, Lange K (2009) Fast model-based estimation of
747 ancestry in unrelated individuals. Genome research 19:1655-1664
748 40. Price AL, Zaitlen NA, Reich D, Patterson N (2010) New approaches to population
749 stratification in genome-wide association studies. Nature reviews. Genetics 11:459-463
750 41. Mathieson I, Mcvean G (2014) Demography and the Age of Rare Variants. 10
751 42. O'Connor TD, Fu W, Mychaleckyj JC, Logsdon B, Auer P, Carlson CS, Leal SM,
752 Smith JD, Rieder MJ, Bamshad MJ, et al (2015) Rare variation facilitates inferences of
753 fine-scale population structure in humans. Mol Biol Evol 32:653-660
754 43. Babron MC, de Tayrac M, Rutledge DN, Zeggini E, Génin E (2012) Rare and low
755 frequency variant stratification in the UK population: description and impact on
756 association tests. PLoS One 7:e46519

757 44. Bhatia G, Gusev A, Loh P-R, Finucane HK, Vilhjalmsson BJ, Ripke S, Purcell S,
758 Stahl E, Daly M, de Candia TR (2016) Subtle stratification confounds estimates of
759 heritability from rare variants. bioRxiv:048181
760 45. Szulc P, Bogdan M, Frommlet F, Tang H (2016) Joint Genotype-and Ancestry-
761 based Genome-wide Association Studies in Admixed Populations. bioRxiv:062554
762 46. Conomos M, Reiner A, Weir B, Thornton T (2016) Model-free Estimation of Recent
763 Genetic Relatedness. The American Journal of Human Genetics 98:127-148
764 47. Zaitlen N, Paşaniuc B, Gur T, Ziv E, Halperin E (2010) Leveraging genetic variability
765 across populations for the identification of causal variants. Am J Hum Genet 86:23-33
766 48. Genovese G, Handsaker RE, Li H, Kenny EE, McCarroll SA (2013) Mapping the
767 human reference genome's missing sequence by three-way admixture in Latino
768 genomes. Am J Hum Genet 93:411-421
769 49. Baharian S, Barakatt M, Gignoux CR, Shringarpure S, Errington J, Blot WJ,
770 Bustamante CD, Kenny EE, Williams SM, Aldrich MC, et al (2016) The Great Migration
771 and African-American Genomic Diversity. PLoS genetics 12:e1006059
772 50. Reich D, Patterson N, Campbell D, Tandon A, Mazieres S, Ray N, Parra MV, Rojas
773 W, Duque C, Mesa N, et al (2012) Reconstructing Native American population history.
774 Nature 488:370-374
775 51. Ruiz-Linares A, Adhikari K, Acuña-Alonzo V, Quinto-Sanchez M, Jaramillo C, Arias
776 W, Fuentes M, Pizarro M, Everardo P, de Avila F, et al (2014) Admixture in Latin
777 America: geographic structure, phenotypic diversity and self-perception of ancestry
778 based on 7,342 individuals. PLoS Genet 10:e1004572

52. Moreno-Estrada A, Gignoux CR, Fernández-López JC, Zakharia F, Sikora M, Contreras AV, Acuña-Alonzo V, Sandoval K, Eng C, Romero-Hidalgo S, et al (2014) The genetics of Mexico recapitulates Native American substructure and affects biomedical traits. Science (New York, N.Y.) 344:1280-1285

53. Vilhjálmsson BJ, Yang J, Finucane HK, Gusev A, Lindström S, Ripke S, Genovese G, Loh PR, Bhatia G, Do R, et al (2015) Modeling Linkage Disequilibrium Increases Accuracy of Polygenic Risk Scores. Am J Hum Genet 97:576-592

54. Mao X, Bigham AW, Mei R, Gutierrez G, Weiss KM, Brutsaert TD, Leon-Velarde F, Moore LG, Vargas E, McKeigue PM, et al (2007) A genomewide admixture mapping panel for Hispanic/Latino populations. American journal of human genetics 80:1171-1178

55. O'Connell J, Gurdasani D, Delaneau O, Pirastu N, Ulivi S, Cocca M, Traglia M, Huang J, Huffman JE, Rudan I, McQuillan R, et al (2014) A General Approach for Haplotype Phasing across the Full Spectrum of Relatedness. PLoS Genetics 10:e1004234

56. Maples BK, Gravel S, Kenny EE, Bustamante CD (2013) RFMix: A Discriminative Modeling Approach for Rapid and Robust Local-Ancestry Inference. American journal of human genetics 93:278-288

57. Gravel S (2012) Population genetics models of local ancestry. Genetics 191:607-619

58. 1000 Genomes Project Consortium (2012) An integrated map of genetic variation from 1,092 human genomes. Nature 135:0-9

801 59. Purcell S, Neale B, Toddbrown K, Thomas L, Ferreira M, Bender D, Maller J, Sklar
802 P, Debakker P, Daly M (2007) PLINK: A Tool Set for Whole-Genome Association and
803 Population-Based Linkage Analyses. The American Journal of Human Genetics 81:559-
804 575
805 60. Kelleher J, Etheridge AM, McVean G (2016) Efficient coalescent simulation and
806 genealogical analysis for large sample sizes. PLoS Comput Biol 12:e1004842
807 61. Mathias RA, Taub MA, Gignoux CR, Fu W, Musharoff S, O'Connor TD, Vergara C,
808 Torgerson DG, Pino-Yanes M, Shringarpure SS, et al (2016) A continuum of admixture
809 in the Western Hemisphere revealed by the African Diaspora genome. Nature
810 Communications 7:12522
811 62. Shringarpure SS, Bustamante CD, Lange KL, Alexander DH (2016) Efficient
812 analysis of large datasets and sex bias with ADMIXTURE. bioarXiv 1:1-10
813 63. Price AL, Patterson NJ, Plenge RM, Weinblatt ME, Shadick NA, Reich D (2006)
814 Principal components analysis corrects for stratification in genome-wide association
815 studies. Nature genetics 38:904-909
816 64. Baran Y, Pasaniuc B, Sankararaman S, Torgerson DG, Gignoux C, Eng C,
817 Rodriguez-Cintron W, Chapela R, Ford JG, Avila PC, et al (2012) Fast and accurate
818 inference of local ancestry in Latino populations. Bioinformatics 28:1359-1367
819 65. Moreno-Estrada A, Gravel S, Zakharia F, McCauley JL, Byrnes JK, Gignoux CR,
820 Ortiz-Tello PA, Martínez RJ, Hedges DJ, Morris RW, et al (2013) Reconstructing the
821 Population Genetic History of the Caribbean. PLoS Genetics 9:e1003925

822 66. Moreno-Estrada A, Gravel S, Zakharia F, McCauley JL, Byrnes JK, Gignoux CR,
823 Ortiz-Tello PA, Martínez RJ, Hedges DJ, Morris RW, et al (2013) Reconstructing the
824 Population Genetic History of the Caribbean. PLoS Genetics 9:e1003925
825 67. Tishkoff SA, Reed FA, Friedlaender FR, Ehret C, Ranciaro A, Froment A, Hirbo JB,
826 Awomoyi AA, Bodo J, Doumbo O, et al (2009) The genetic structure and history of
827 Africans and African Americans. Science (New York, N.Y.) 324:1035-1044
828 68. Zakharia F, Basu A, Absher D, Assimes TL, Go AS, Hlatky MA, Iribarren C, Knowles
829 JW, Li J, Narasimhan B, et al (2009) Characterizing the admixed African ancestry of
830 African Americans. Genome biology 10:R141
831 69. Schroeder H, Ávila-Arcos MC, Malaspinas A, Poznik GD, Sandoval-Velasco M,
832 Carpenter ML, Moreno-Mayar JV, Sikora M, Johnson PLF, Allentoft ME, et al (2015)
833 Genome-wide ancestry of 17th-century enslaved Africans from the Caribbean.
834 Proceedings of the National Academy of Sciences 112:201421784
835 70. Gravel S, Zakharia F, Moreno-Estrada A, Byrnes JK, Muzzio M, Rodriguez-Flores
836 JL, Kenny EE, Gignoux CR, Maples BK, Guiblet W, et al (2013) Reconstructing Native
837 American migrations from whole-genome and whole-exome data. PLoS genetics
838 9:e1004023
839 71. Kessler MD, Yerges-Armstrong L, Taub MA, Shetty AC, Maloney K, Jeng LJB,
840 Ruczinski I, Levin AM, Williams LK, Beaty TH, et al (2016) Challenges and disparities in
841 the application of personalized genomic medicine to populations with African ancestry.
842 Nature Communications 7:12521

843 72. Purcell SM, Wray NR, Stone JL, Visscher PM, O'Donovan MC, Sullivan PF, Sklar P,
844 Purcell SM, Stone JL, Sullivan PF, et al (2009) Common polygenic variation contributes
845 to risk of schizophrenia and bipolar disorder. Nature
846 73. Shungin D, Winkler TW, Croteau-Chonka DC, Ferreira T, Locke AE, Mägi R,
847 Strawbridge RJ, Pers TH, Fischer K, Justice AE, et al (2015) New genetic loci link
848 adipose and insulin biology to body fat distribution. Nature 518:187-196
849 74. Gaulton KJ, Ferreira T, Lee Y, Raimondo A, Mägi R, Reschen ME, Mahajan A,
850 Locke A, Rayner NW, Robertson N, et al (2015) Genetic fine mapping and genomic
851 annotation defines causal mechanisms at type 2 diabetes susceptibility loci. Nat Genet
852 47:1415-1425
853 75. Mahajan A, Go MJ, Zhang W, Below JE, Gaulton KJ, Ferreira T, Horikoshi M,
854 Johnson AD, Ng MC, Prokopenko I, et al (2014) Genome-wide trans-ancestry meta-
855 analysis provides insight into the genetic architecture of type 2 diabetes susceptibility.
856 Nat Genet 46:234-244
857 76. Moffatt MF, Gut IG, Demenais F, Strachan DP, Bouzigon E, Heath S, Von Mutius E,
858 Farrall M, Lathrop M, Cookson WO (2010) A large-scale, consortium-based
859 genomewide association study of asthma. New England Journal of Medicine 363:1211-
860 1221
861 77. N'Diaye A, Chen GK, Palmer CD, Ge B, Tayo B, Mathias RA, Ding J, Nalls MA,
862 Adeyemo A, Adoue V, et al (2011) Identification, replication, and fine-mapping of Loci
863 associated with adult height in individuals of african ancestry. PLoS Genet 7:e1002298
864 78. Gustafsson A, Lindenfors P (2004) Human size evolution: no evolutionary allometric
865 relationship between male and female stature. J Hum Evol 47:253-266

866 79. Whiteford HA, Degenhardt L, Rehm J, Baxter AJ, Ferrari AJ, Erskine HE, Charlson
867 FJ, Norman RE, Flaxman AD, Johns N, et al (2013) Global burden of disease
868 attributable to mental and substance use disorders: findings from the Global Burden of
869 Disease Study 2010. The Lancet 382:1575-1586
870 80. De Candia TR, Lee SH, Yang J, Browning BL, Gejman PV, Levinson DF, Mowry BJ,
871 Hewitt JK, Goddard ME, O'Donovan MC, et al (2013) Additive genetic variation in
872 schizophrenia risk is shared by populations of African and European descent. American
873 Journal of Human Genetics 93:463-470
874 81. Lango Allen H, Estrada K, Lettre G, Berndt SI, Weedon MN, Rivadeneira F, Willer
875 CJ, Jackson AU, Vedantam S, Raychaudhuri S, et al (2010) Hundreds of variants
876 clustered in genomic loci and biological pathways affect human height. Nature 467:832-
877 838
878 82. Chan Y, Lim E, Sandholm N, Wang S, McKnight A, Ripke S, Daly M, Neale B,
879 Salem R, Hirschhorn J (2014) An Excess of Risk-Increasing Low-Frequency Variants
880 Can Be a Signal of Polygenic Inheritance in Complex Diseases. The American Journal
881 of Human Genetics 94:437-452
882 83. Minikel EV, Vallabh SM, Lek M, Estrada K, Samocha KE, Sathirapongsasuti JF,
883 McLean CY, Tung JY, Yu LPC, Gambetti P, et al (2016) Quantifying prion disease
884 penetrance using large population control cohorts. Science Translational Medicine
885 8:322ra9-322ra9
886 84. Walsh R, Thomson K, Ware JS, Funke BH, Woodley J, McGuire KJ, Mazzarotto F,
887 Blair E, Seller A, Taylor JC (2016) Reassessment of Mendelian gene pathogenicity
888 using 7,855 cardiomyopathy cases and 60,706 reference samples. bioRxiv:041111

889 85. Manrai AK, Funke BH, Rehm HL, Olesen MS, Maron BA, Szolovits P, Margulies
890 DM, Loscalzo J, Kohane IS (2016) Genetic Misdiagnoses and the Potential for Health
891 Disparities. New England Journal of Medicine 375:655-665
892 86. Li YR, Keating BJ (2014) Trans-ethnic genome-wide association studies:
893 advantages and challenges of mapping in diverse populations. Genome Med 6:91
894 87. Dumitrescu L, Carty CL, Taylor K, Schumacher FR, Hindorff LA, Ambite JL,
895 Anderson G, Best LG, Brown-Gentry K, Bůžková P, et al (2011) Genetic Determinants
896 of Lipid Traits in Diverse Populations from the Population Architecture using Genomics
897 and Epidemiology (PAGE) Study. PLoS Genetics 7:e1002138
898 88. Freedman ML, Haiman CA, Patterson N, McDonald GJ, Tandon A, Waliszewska A,
899 Penney K, Steen RG, Ardlie K, John EM (2006) Admixture mapping identifies 8q24 as a
900 prostate cancer risk locus in African-American men. Proceedings of the National
901 Academy of Sciences 103:14068-14073
902 89. Rosenberg NA, Huang L, Jewett EM, Szpiech ZA, Jankovic I, Boehnke M (2010)
903 Genome-wide association studies in diverse populations. Nature reviews. Genetics
904 11:356-366
905 90. Dudbridge F (2013) Power and predictive accuracy of polygenic risk scores. PLoS
906 Genet 9:e1003348
907 91. Wray NR, Yang J, Hayes BJ, Price AL, Goddard ME, Visscher PM (2013) Pitfalls of
908 predicting complex traits from SNPs. Nature Reviews Genetics 14:507-515
909
910